

$L_{2,3}$ edge of silicon: Theory and experiment

P. Aebi, J. Keller,* M. Erbudak, and F. Vanini

Institut für Angewandte Physik, Eidgenössische Technische Hochschule—Zürich, CH-8093 Zürich, Switzerland

(Received 19 February 1988)

Structures in the electron-energy-loss spectrum up to 30 eV above the $L_{2,3}$ edge of clean silicon, excited with high- and low-energy electrons, are found to be in good agreement with a multiple-scattering calculation of the empty density of states of a tetrahedral cluster of 17 silicon atoms. The relaxation of the excited atom is investigated by means of the emission spectrum. The decay channels involving electrons in resonant scattering states produce high-energy satellites to the conventional Auger transition in accordance with the excitation spectrum.

I. INTRODUCTION

Computations of the electronic density of states (DOS) of solids have been limited in the past either to the occupied bands or to states near the Fermi level, E_F , according to the needs of available spectroscopic results, e.g., photoemission, reflectivity, etc. With the emergence of the experimental procedures probing unoccupied states far above E_F , such as bremsstrahlung isochromat spectroscopy (BIS) or x-ray-absorption spectroscopy, computations have been extended to such states.¹ Electron-energy-loss spectroscopy (EELS) yields information on the initial and final states and the matrix elements coupling them. Hence, such experiments need the support of the theoretical DOS and the transition matrix elements, where the matrix elements weigh the transitions to different angular-momentum channels. For the excitation of core states, mainly the unoccupied DOS has been investigated; modulations measured above the core edges are the basis of XANES (x-ray-absorption near-edge structure) and EXAFS (extended x-ray-absorption fine structure) used for structural investigation of the local environment of atoms in a solid. Owing to the growing mean free path of the electrons excited above E_F going from the EXAFS to the XANES regime, interference with the outgoing electron wave is not only due to single backscattering at the neighbors of the excited atom, but also to scattering at several centers [multiple scattering (MS)]. For the excitation of the inner shells, mostly x rays from a synchrotron-radiation source have been used. EXAFS-like modulations have also been reported in EELS with high-energy electrons (300 keV) in transmission² and with low-energy (1–2 keV) electrons in reflection³ experiments.

The recombination of excited core levels results in Auger and/or Coster-Kronig transitions with well-defined emission energies. For some elements structures above the Auger transition have been investigated. Those observed on the high-energy side of the Cu $3pVV$ Auger transition⁴ have been attributed to EXAFS-like processes.⁵ On the other hand, similar structures observed in a limited energy range above the silicon $2pVV$ Auger transition have been attributed by some authors to plasmon gain⁶ and by others to double-ionization⁷ pro-

cesses. It is not yet clear why, with excitation by low-energy electrons, some materials show strong modulations in the EXAFS region above the core edges or beyond the CVV Auger transitions and others do not at all. Therefore, it is useful to investigate the near-edge region, where not only information on neighbor distances is present as in the extended fine-structure region, but also on bond angles because of MS paths.⁸ The aim of this report is to contribute towards the understanding the structures above the Si $2p$ edge and the Si $2pVV$ Auger transition, as it has been shown that in Si a strong similarity exists between near-edge structures obtained by conventional methods and those investigated with low-energy electrons.⁹ Furthermore, Si has been chosen as an example of a material which does not show modulations in the EXAFS region. A self-consistent MS calculation has been performed for a tetrahedral cluster of 17 Si atoms to obtain the scattering channels in the conduction band and several eV above it. Clusters of 17 scatterers have been chosen to include the nearest and next-nearest neighbors. The inclusion of the third-nearest neighbors requires a cluster of 29 scatterers; this would considerably increase the computer time. Results are compared with EELS data, obtained with an excitation energy of 450 eV, and published data from high-energy electron excitation.¹⁰ The structures above the $2pVV$ Auger transition are identical as an autoionization emission from a partly relaxed Si atom. In Secs. II and III experimental and theoretical procedures are outlined. Results are reported in Sec. IV. Discussion and conclusions follow in Secs. V and VI.

II. EXPERIMENT

The experiments were performed in an ultrahigh-vacuum apparatus with a total pressure in the 10^{-9} -Pa range. Silicon wafers with (100) faces (B doped, 5 Ω cm) were chemically etched before insertion into the vacuum chamber. Final surface preparation was achieved by sputtering (Ar^+ , 2750 eV; $1 \mu\text{A mm}^{-2}$) and annealing (1200 K) cycles until no trace of C and O contamination could be detected by Auger-electron spectroscopy. The annealing temperature was chosen high enough to guarantee the recrystallization of the sputtered surfaces.

Positive ions for sputtering and electrons are produced by means of a hybrid gun.¹¹ A single-stage cylindrical mirror analyzer with a resolution of $\Delta E/E=0.004$ and a high-current channeltron are employed to detect the secondary electrons. The axis of the gun and of the analyzer are aligned perpendicular to each other. The electron incidence was along the surface normal. The EELS measurement was recorded with a primary electron energy of 450 eV in order to keep the total energy resolution near the $L_{2,3}$ edge at about 2 eV. The Auger intensity was measured using a primary electron energy of 1 keV to increase the intensity of the primary beam and hence the intensity of emitted Auger electrons. The EELS spectrum was recorded in the negative second-derivative mode employing a phase-sensitive amplifier and modulating the potential of the outer cylinder of the analyzer with 1.4 V peak to peak. The registration of the second derivative eliminates the background of secondary electrons up to a quadratic contribution that otherwise constitutes a severe limitation to electron-excited spectroscopies. Since the second derivative is the inverse of the radius of curvature of the original function, the extrema are inherently at the same energy position. The Auger intensity was recorded both in the integral and in the second-derivative form. Further details of the experiment have been communicated before.¹²

III. THEORY

A cellular MS technique¹³ has been used to calculate the empty density of states. The model material was a tetrahedral cluster of 17 silicon atoms in the diamond structure with a lattice constant of 10.2612 atomic units (a.u.) = 5.43 Å immersed in the spherical average potential of the rest of the system. In a.u. the local MS DOS $\rho_i(\mathbf{r}; E)$ for the atom i at energy E is given by the integration over the cell i of the diagonal elements of the imaginary part of the Green's function,

$$-\frac{1}{\pi} \int_i d\mathbf{r} \langle \langle \mathbf{r} | \text{Im} G^+(E) | \mathbf{r} \rangle \rangle_i = \int \rho_i(\mathbf{r}; E) d\mathbf{r}, \quad (1)$$

where the $\langle \langle \dots \rangle \rangle_i$ denotes a configurational average with the atom i fixed. The G^+ matrix of the system is given in terms of the free electron Green's function G_0^+ as

$$G^+ = G_0^+ / (1 - G_0^+ K). \quad (2)$$

K being the single-site scattering matrix for stationary-wave boundary conditions. G^+ can be expressed in a supermatrix angular-momentum representation (\tilde{G}^+) as

$$\tilde{G}_{iL, jL'}^+ = \sum_{k, L''} \tilde{G}_{0iL, kL''}^+ [(1 - \tilde{G}_0^+ K)^{-1}]_{kL'', jL'}. \quad (3)$$

L is the ordered pair (l, m) and i, j, k , denote scatterer atoms. The radial local density of states can be written in terms of (3) with $\langle \langle \dots \rangle \rangle_{\text{sp}}$ denoting a spherical average

$$\begin{aligned} \rho(r'_i; E) &= -\frac{1}{\pi} \langle \langle \mathbf{r}' | \text{Im} G^+ | \mathbf{r}' \rangle \rangle_{\text{sp}} \\ &= -4 \sum_L R_l^2(r'_i; E) \text{Im} \tilde{G}_{li, li}^+, \end{aligned} \quad (4)$$

where $r' = |\mathbf{r}'| = |\mathbf{r} - \mathbf{r}_i|$ and the $R_l(r'_i; E)$ are the solutions for energy E of the radial Schrödinger equation for atom i in the atomic potential $V(r')$ with the boundary condition

$$R_l(r'_i; E) = j_l(\kappa r'_i) \cos \eta_l - n_l(\kappa r'_i) \sin \eta_l.$$

The potential is computed by superimposing the free-atom charge density obtained from a relativistic self-consistent statistical $X\alpha$ exchange calculation¹³ to the central cell of a 14-shell cluster.

IV. RESULTS

Figure 1 compares the calculated empty MS DOS with EELS results on the silicon $L_{2,3}$ edge. The curve labeled A is the energy-loss spectrum of electrons with a primary energy of 450 eV recorded in the second-derivative mode. Curves s , p , d , and f are the calculated empty MS DOS contributions, corresponding to angular-momentum-scattering paths with $l=0, 1, 2$, and 3 , respectively. All four curves have the same ordinate scale. Curve B shows, in the integral mode, the energy-loss spectrum of high-energy electrons obtained from a Si film a few hundred Å thick.¹⁰ The abscissa represents the energy loss for curves A and B . All curves are aligned to coincide at

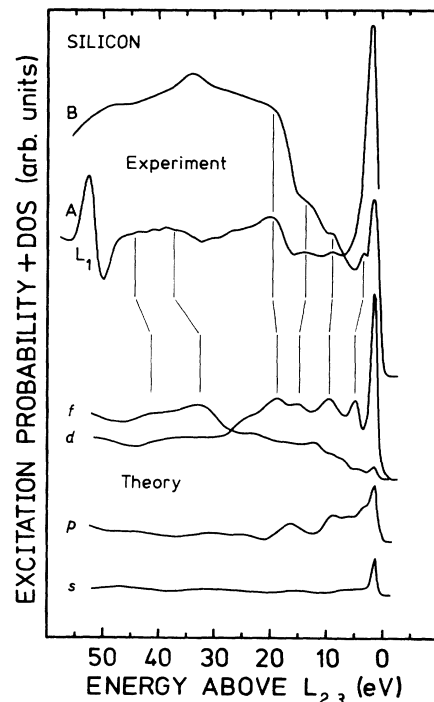


FIG. 1. Reflection EELS results from Si(100) at an excitation energy of 450 eV (curve A) are compared with those of a transmission experiment (Ref. 10) using high-energy electrons on a crystalline Si film (curve B). Calculated l -projected empty MS DOS are displayed as curves s , p , d , and f where the labels denote the angular momentum $l=0, 1, 2$, and 3 . The abscissa gives the energy in eV relative to the $L_{2,3}$ core-excitation threshold. Curve A is taken in the negative second derivative.

the bottom of the conduction band. Vertical lines are drawn to indicate common features. The excitation of the L_1 edge is observed at about 50 eV: Curve *A* shows a sharp transition, while in curve *B* it is only represented as a faint shoulder.

The comparison between theory and experiment shows that up to 30 eV the empty DOS is dominated by the scattering paths with d angular-momentum character. Here, all features in *A* and *B* are in good agreement with calculations within a difference of smaller than 2 eV. For higher energy losses the largest contribution stems from f -like scattering. In this region, the EELS data show discrepancies, and the differences grow up to 3.7 eV. The remaining difference in the background is due to the fact that *A* is measured in the second-derivative mode, eliminating background up to a quadratic contribution.

Figure 2 shows the high-energy leading edge of the Si $2pVV$ Auger transition intensity (curve *A*) and its negative second derivative (curve *A'*) which reveals latent structures. Also shown is curve *A* in 35-fold amplification. The energy scale is corrected for the work function of the analyzer. Since the EELS spectrum contains different excitation channels and the Auger transitions represent the relaxation processes of the excited atom, it is appropriate to compare the Auger spectrum with the corresponding EELS data (curve *A* in Fig. 1); the latter is shown here in curve *C*. The positioning of the energy scale is not straightforward if electron correla-

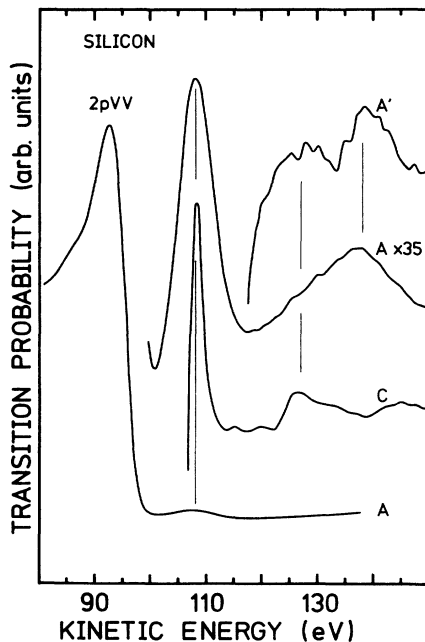


FIG. 2. Spectrum of the silicon $2pVV$ Auger transition intensity and its high-energy satellite (curve *A*) with its 35-fold amplification [(curve *A*) \times 35] measured in the integral mode. Curve *A'* shows the measured negative second derivative. The measured $2p$ edge, as shown in Fig. 1, curve *A*, is plotted as curve *C* aligned to the main structure above the $2pVV$ Auger transition (see text).

tions are not neglected. In the figure, the $2p$ edge in curve *C* is aligned with the main feature above the $2pVV$ transition; a tentative justification of this procedure is given in the next section. This allows agreement in the position of structures in curves *A'* and *C* (both second-derivative spectra) at 126 eV.

V. DISCUSSION

The understanding of the Si $L_{2,3}$ absorption edge was initiated by Gaehwiler and Brown,¹⁴ who performed photoabsorption experiments near the $2p$ edge of Si using synchrotron radiation. Their analysis, employing one-electron band theory, failed to account for the observed structures. Later, Ritsko *et al.*¹⁵ performed a calculation adding to the free-electron absorption an EXAFS-like contribution due to the crystal structure. They attributed the broad background observed in the high-energy EELS (Fig. 1, curve *B*) mainly to the free-electron absorption, ignoring backscattering.¹⁶

In electron-excited transitions the dipole approximation is valid if $qr \ll 1$, where r is the radius of the excited core and q the momentum transfer. The transition probability, then, in a single-particle formalism, is proportional to an energy-dependent matrix element times a projected empty DOS with appropriate symmetry. The criterion for the dipole approximation is fulfilled for the results represented as curve *B* in Fig. 1, but certainly not for curve *A*. Nevertheless, the agreement of prominent structures is striking. Therefore, this agreement of both spectra can be explained by the dominant d part of the empty MS DOS which is mainly probed by the absorption experiments. In the energy-loss region above 30 eV, where the f part is dominant, agreement becomes poorer. Also, the L_1 edge in *A* manifests the occurrence of transitions other than of dipole type, whereas in *B* the small empty p DOS limits the transition probability. Discrepancies in energy between the calculated partial DOS and the experiment are attributed to the energy dependence of the ground-state potential¹⁷ as observed in BIS (Ref. 18) and x-ray-absorption measurements,¹⁹ and to the fact that we have neglected matrix elements leading to final scattering states of different symmetry, since mixing can produce a slight shift of the energy position. The cellular MS technique is able to treat itinerant and localized states with equal precision.¹³ This is achieved for the occupied bands by performing a large number of calculations with different assumed configurations in order to find self-consistently the occupation of the f bands. In the present work, the unoccupied f bands are calculated. EELS results, however, depend on the difference of the total energy of the system before and after the excitation process, where there is an electron in the final state occupying the f band. Since the f -level eigenvalues depend strongly on occupation, the discrepancy between the measurements and calculations above 30 eV can be due to such final-state effects. Furthermore, changing the lattice constant of the tetrahedral cluster shifts the energy positions of the maxima.²⁰ Several calculations have been performed allowing contraction and expansion of the diamond cluster up to 10%. The results presented

here for an unrelaxed lattice produce the best fit for the structures in the near-edge region up to 30 eV.

The Si $2pVV$ Auger transition (Fig. 2, curve *A*) shows several structures on the high-energy side. In the past, the main structure at 108 eV has been attributed either to the $2pVV$ emission with a double-ionized initial state⁷ or to a plasmon gain of emitted Auger electrons.⁶ In the light of the present calculations, an alternative explanation is possible. Whereas in the initial state of a conventional Auger process a $2p$ electron is excited to infinity, in the case of electron excitation there is a nonvanishing probability that it occupies a resonant scattering state above E_F . This electron can then participate in the recombination of the core hole, producing satellite lines to Auger transitions, known as autoionization emission in the case of isolated atoms²¹ and transition metals.¹² The density of the MS channels where an excited electron can resonantly be trapped is represented by the empty DOS in Fig. 1. In order to estimate the energy difference between the Auger and the autoionization emission, one has to consider the initial and final states of the two processes; in the conventional Auger process the initial state is $2p^53(sp)^4$ and the final state is $2p^63(sp)^2$. For the autoionization process the initial state is $2p^53(sp)^43d^1$, the additional electron occupying the otherwise empty d state. This is possible because of the large empty MS DOS with d symmetry and the allowed dipole transitions from p to d symmetry. Then, the final state is a single hole in the valence band: $2p^63(sp)^3$. We have calculated the total energies of all four states using a relativistic self-consistent-field program with Wigner-Seitz boundary conditions with a radius of 3 a.u. ($= 1.588 \text{ \AA}$) in order to estimate the emission energies of the two processes. Both initial-state energies were calculated in the self-consistently computed potential of neutral silicon with the same boundary conditions, i.e., the initial states are not relaxed. For the final states the calculation was done once fully relaxed, i.e., until self-consistency is reached, and once not relaxed. In the conventional Auger transition, this gives rise to a difference in energy of up to 25 eV between the relaxed and the unrelaxed final state, and in the autoionization the difference is less than 7 eV. If one chooses arbitrarily a degree of relaxation of 70% for the final states, the emission energies of the electron in the two cases are 92 and 108 eV, which is in excellent agreement with the measured data. This estimation justifies our alignment of the loss spectrum with the autoionization-emission resonance.

Two further structures are present in the second-derivative curve (*A'*) beyond the autoionization emis-

sion: The first corresponds to that in the loss spectrum, while the second is attributed to the $2sVV$ Auger transitions.

VI. CONCLUSION

We have presented a comparison between EELS data above the $L_{2,3}$ edge of silicon and a MS calculation of the empty DOS. The agreement between the EELS spectra and the computed MS DOS is very good in an energy range up to 30 eV above the $L_{2,3}$ edge. Thus the near-edge structures above the Si $L_{2,3}$ edge can be assigned to the transition of a $2p$ core electron into empty MS channels with d character. Beyond 30 eV the spectral shape can be accounted for by the p - f transitions, which are not forbidden under the present experimental conditions. No attempt was made to calculate higher-order l components of the DOS since the matrix elements for transitions into such states are very small. An alternative explanation for the high-energy satellite to the main $2pVV$ Auger line is given in terms of excited electrons participating in the Auger transition. Thus the decay of the MS resonances are observed in the emission spectrum; this is consistent with an autoionization process. An estimate of the satellite energy requires a partial relaxation of the silicon atom. Structures above the conduction-band edge have been measured in BIS experiments,²² which resemble closely the present results. As a result, we conclude that the EELS with low-energy primary electrons in the reflection mode offers a useful tool for probing the local geometry around the excited atom by means of the MS channels. Nevertheless, if more than a single symmetry is dominant in the empty MS DOS, matrix elements for transitions into different l components have to be considered. In this work, it is found that the computations for an unrelaxed lattice reproduce the measured spectra best. In order to obtain detailed information about the surface structure of Si(100), further calculations with clusters representing a surface geometry with partially relaxed surface atoms have to be performed.

ACKNOWLEDGMENTS

One of us (J.K.) is grateful for the hospitality of the Institut für Angewandte Physik, Eidgenössische Technische Hochschule-Zürich. The authors are indebted to G. Kosterz for his continuous interest and useful comments on the manuscript. Helpful discussions with F. Mila and technical help by A. Meier are acknowledged. This work was supported in part by the Schweizerischer Nationalfonds zur Förderung der Wissenschaften.

*Permanent address: Facultad de Química, Universidad Nacional Autónoma de México, Apartado 70-528, 04510 México, Distrito Federal, México.

¹See, e.g., W. Speier, J. C. Fuggle, R. Zeller, B. Ackermann, K. Szot, K. U. Hillebrecht, and M. Campagna, Phys. Rev. B **30**, 6921 (1984), and references therein.

²*EXAFS Spectroscopy: Techniques and Applications*, edited by B.

K. Teo and D. Joy (Plenum, New York, 1981).

³M. De Crescenzi and G. Chiarello, J. Phys. C **18**, 3595 (1985).

⁴L. McDonnell, B. D. Powell, and D. P. Woodruff, Surf. Sci. **40**, 669 (1973).

⁵M. De Crescenzi, E. Chainet, and J. Derrien, Solid State Commun. **57**, 487 (1986).

⁶M. F. Chung and L. H. Jenkins, Surf. Sci. **26**, 649 (1971).

- ⁷M. Salmerón, A. M. Baró, and J. M. Rojo, *Surf. Sci.* **41**, 11 (1974).
- ⁸A. Bianconi, M. Dell'Ariceia, P. J. Durham, and J. P. Pendry, *Phys. Rev. B* **26**, 6502 (1982).
- ⁹M. Erbudak, P. Aebi, F. Vanini, and G. Kostorz, *J. Electron Spectrosc. Relat. Phenom.* (to be published).
- ¹⁰S. E. Schnatterly, in *Solid State Physics*, edited by H. Ehrenreich, F. Seitz, and D. Turnbull (Academic, New York, 1979), Vol. 34, p. 275.
- ¹¹E. B. Bas, E. Gisler, and F. Stucki, *J. Phys. E* **17**, 405 (1984).
- ¹²A. Cornaz, M. Erbudak, P. Aebi, F. Stucki, and F. Vanini, *Phys. Rev. B* **35**, 3062 (1987).
- ¹³J. Keller, in *Computational Methods for Large Molecules and Localized States in Solids*, edited by F. Herman, A. D. McLean, and R. K. Nesbitt (Plenum, New York, 1972), p. 341; R. Evans and J. Keller, *J. Phys. C* **4**, 3155 (1971); J. Keller and P. V. Smith, *ibid.* **5**, 1109 (1972); J. Keller, C. Amador, and C. de Teresa, *Rev. Mex. Fis.* **30**, 447 (1984); T. L. Loucks, *Augmented Plane Wave Method* (Benjamin, New York, 1967); M. Castro, J. Keller, and P. Rius, *Hyperfine Interact.* **12**, 261 (1982).
- ¹⁴C. Gäwiller and F. C. Brown, *Phys. Rev. B* **2**, 1918 (1970).
- ¹⁵J. J. Ritsko, S. E. Schnatterly, and P. C. Gibbons, *Phys. Rev. Lett.* **32**, 671 (1974).
- ¹⁶The second-derivative mode employed here offers the possibility to observe mainly the part due to the crystal structure.
- ¹⁷L. Hedin and B. I. Lundqvist, *J. Phys. C* **4**, 2064 (1971).
- ¹⁸W. Speier, J. C. Fuggle, R. Zeller, and M. Campagna, in *EXAFS and Near Edge Structure III*, edited by K. O. Hodgson, B. Hedman, and J. E. Penner-Hahn (Springer, New York, 1984), p. 496.
- ¹⁹G. Materlik, J. E. Müller, and J. W. Wilkins, *Phys. Rev. Lett.* **50**, 267 (1983).
- ²⁰C. R. Natoli, in *EXAFS and Near Edge Structure*, Vol. 27 of *Springer Series in Chemical Physics*, edited by A. Bianconi, L. Incoccia, and S. Stipcich (Springer, New York, 1983), p. 43.
- ²¹M. O. Krause, T. A. Carlson, and W. E. Moddeman, *J. Phys. (Paris) Colloq.* **32**, C4-139 (1971).
- ²²H. J. M. Hoekstra, W. Speier, R. Zeller, and J. C. Fuggle, *Phys. Rev. B* **34**, 5177 (1986).